ACS APPLIED MATERIALS & INTERFACES

Research Article

www.acsami.org

Complex Internal Bias Fields in Ferroelectric Hafnium Oxide

Tony Schenk,*[,†] Michael Hoffmann,[†] Johannes Ocker,[†] Milan Pešić,[†] Thomas Mikolajick,[†,‡] and Uwe Schroeder[†]

[†]NaMLab gGmbH, Noethnitzer Strasse 64, D-01187 Dresden, Germany

[‡]Chair of Nanoelectronic Materials, TU Dresden, D-01062 Dresden, Germany

ABSTRACT: For the rather new hafnia- and zirconia-based ferroelectrics, a lot of questions are still unsettled. Among them is the electric field cycling behavior consisting of (1) wake-up, (2) fatigue, and (3) the recently discovered subcycling-induced split-up/merging effect of transient current peaks in a hysteresis measurement. In the present work, first-order reversal curves (FORCs) are applied to study the evolution of the switching and backswitching field distribution within the frame of the Preisach model for three different phenomena: (1) The pristine film contains two oppositely biased regions. These internal bias fields vanish during the wake-up cycling. (2) Fatigue as a decrease in the number of switchable domains is accompanied by a slight increase in the mean absolute value of the switching field. (3) The split-up effect is shown to also be related to local bias fields in a complex situation resulting from both the field cycling treatment and the measurement procedure. Moreover, the role of the wake-up phenomenon is discussed with respect to optimizing low-voltage operation conditions of ferroelectric memories toward reasonably high and stable remanent polarization and highest possible endurance.

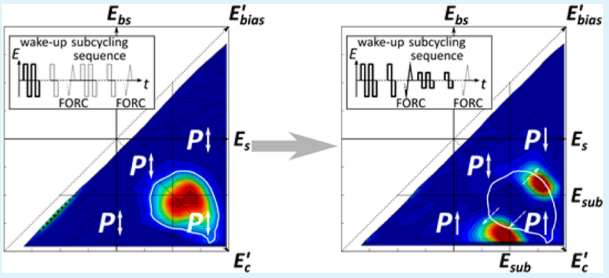

KEYWORDS: *hafnium oxide, ferroelectric, first-order reversal curves, electric field cycling behavior, internal bias fields*

INTRODUCTION

Ferroelectricity in Si-doped HfO_2 thin films was first reported in 2011.[1] In the following years, this behavior was shown for a variety of different dopants[2] and for a solid solution of HfO_2 and ZrO_2.[3,4] This new class of ferroelectrics started attracting attention of both theoretical[5−8] and application oriented[9−13] groups. Nonetheless, the polycrystalline structure of the only some ten nanometers thin films and the variety of rather similar potential hafnia phases hampered the structural analysis. Consequently, it took four years until the question of the structural origin of this unexpected behavior could finally be settled using a combination of scanning transmission electron microscopy and electron diffraction. Sang and co-workers proved the originally claimed orthorhombic $Pca2_1$ (or in a different setting formerly called $Pbc2_1$) as the root of the structural ferroelectricity in Gd:HfO_2.[14] Besides understanding the origin of ferroelectricity, also a comprehensive picture of the evolution of the polarization hysteresis versus continuous switching cycles is crucial. Since this hysteresis is the central property utilized in applications such as ferroelectric memories, it is necessary to know the reasons behind this behavior and how to influence it.

This so-called "electric field cycling behavior" consists of three different phenomena[15] (Figure 1):

(1) "Wake-up": A pristine sample exhibits a pinched hysteresis loop that opens up during electric field cycling and is mostly also accompanied by an increase of the remanent polarization P_r. In conventional ferroelectrics, this is effect is sometimes also called deaging.[16,17]

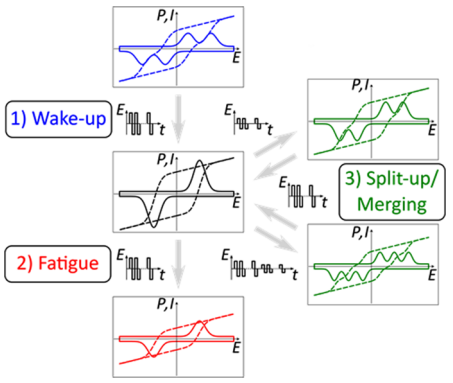

Figure 1. Schematic of the experimental observations for the three phenomena condensed in the term "electric field cycling behavior".

(2) Polarization fatigue: P_r starts gradually decreasing after a certain amount of switching cycles, which is related to a reduced amount of switchable domains. Different reasons such as domain wall pinning and seed inhibition are discussed in the literature.[18]

(3) "Split-up" effect: Subjecting ferroelectric HfO_2 to a certain amount of subcycles, the saturated hysteresis starts to look pinched. In the transient current response, there is a split-up of one original peak into two peaks

Received: June 29, 2015
Accepted: August 26, 2015
Published: August 26, 2015

DOI: 10.1021/acsami.5b05773
ACS Appl. Mater. Interfaces 2015, 7, 20224−20233

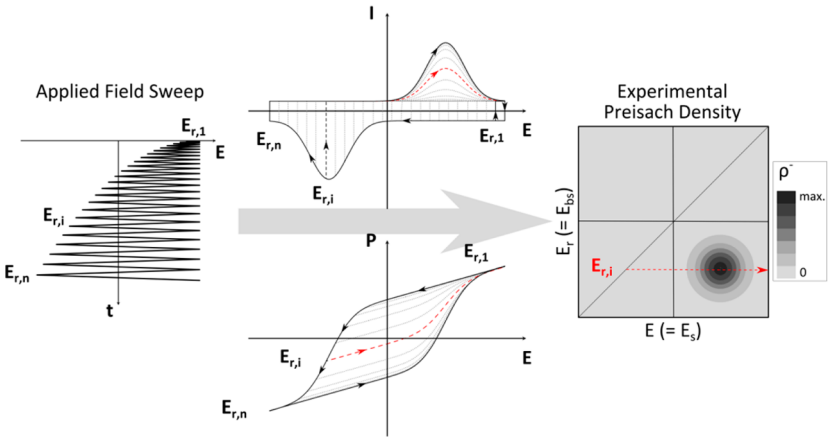

Figure 2. Outline of the first-order reversal curve (FORC) approach: The utilized field sweep from positive saturation to obtain ρ^- (left); the corresponding polarization and transient current loops (middle); calculated experimental Preisach density (right). With the applied field sweep shown on the left, it is possible to calculate one-half of the switching density in the Preisach plane shown on the right. For the depicted version of the field sweep, E equals the switching field E_s and E_r equals the backswitching field E_{bs}. Out of the sweeps from the first reversal field $E_{r,1}$ to the last reversal field $E_{r,n}$, one example was chosen as the i-th curve (red dashed lines) to illustrate how the measurement translates to the obtained switching density plot.

close to the subcycling amplitude. Cycling the sample again with higher amplitude, the split-up vanishes. Moreover, this new phenomenon was reported to be an analogue mechanism and also multiple split-ups at different fields were demonstrated simultaneously. The proposed model capable of explaining all these findings was based on the claim that static (i.e., nonswitching) domains attract defects during the subcycling procedure, which increases the switching field in favor of the switching fields of the nonstatic (i.e., switching) domains.[15]

All three phenomena were studied in this work using a Sr:HfO_2 sample prepared as described earlier.[15] A recent review article summarized potential reasons for deformed hystereses found in literature.[19] It emphasized that the application of first-order reversal curves (FORCs) is a suitable approach to distinguish between several of these potential mechanisms. FORC measurements allow conclusions on the switching field distribution within the frame of the Preisach model.[20] This approach, originally used to characterize magnetic materials,[21] was successfully adapted also to conventional ferroelectrics in the past and described there in more detail.[22,23] Figure 2 shows the procedure of this measurement and the derivation of the switching density ρ^- for the case of probing the reversal fields $E_{r,i}$ in descending order,[23] i.e. by field sweeps starting at positive saturated field region. The central characteristic obtained from this approach is a frequency distribution in the so-called Preisach plane. In the depicted case, it is calculated as the mixed second derivative of the recorded polarization $P^-(E_r,E)$ response of the ascending branches of the field sweeps as follows from eq 1. The easiest numerical calculation of this switching density can be illustrated as follows: For each i-th reversal field $E_{r,i}$ plotted as the y-axis of the Preisach density, the difference in the transient current response to the current response of the previous reversal field $\Delta I(E_{r,i},E) = I(E_{r,i},E) - I(E_{r,i-1},E)$ is plotted versus the field E with $E_r \le E \le E_{max}$, i.e., for the field sweep between the reversal field and the maximum field (positive saturation). Starting from the upper right corner at $E_r = E_{max}$, one horizontal line per E_r step can be drawn into the graph until the complete lower right half below the diagonal $E_r = E$ is filled:

$$\rho^-(E_r, E) = \frac{1}{2}\cdot\frac{\partial^2 P^-_{FORC}(E_r, E)}{\partial E_r \partial E} = \frac{1}{2\cdot\dot{E}}\frac{\partial j^-_{FORC}(E_r, E)}{\partial E_r}$$
$$\approx \frac{1}{2\dot{E}}\frac{j^-_{FORC}(E_{r,i}, E) - j^-_{FORC}(E_{r,i-1}, E)}{E_{r,i} - E_{r,i-1}} \quad (1)$$

So, the change of the switching peak in the current density $j(E_{r,i},E)$ compared to the previous curve $j(E_{r,i-1},E)$ on the ascending field branch toward positive saturation can be traced back to the additional fraction of domains switched to negative polarization (backswitching) by a sweep down to $E_{r,i}$ instead of only to $E_{r,i-1}$. Consequently, a backswitching field $E_{bs} = E_{r,i}$ and a switching field $E_s = E$ (with a precision given by the resolution of the measurement grid) can be attributed to these additional domains. If the depicted field sweep is mirrored at the time axis, the respective switching density can be calculated from the descending branches of the sweep and then called ρ^+ (according to the way of probing $E_{r,i}$ in ascending order). Ideally, ρ^+ and ρ^- should look the same. This switching density (or experimental Preisach density) allows identifying what share of the polarization response has a certain field for switching to positive polarization P (switching field E_s) and negative polarization $-P$ (backswitching field E_{bs}), which cannot be unambiguously extracted from a simple hysteresis measurement.

A coordinate transformation[22,26] as shown in eq 2 can be used to plot the switching density versus the coordinates of coercive field E_c and the bias field E_{bias}, which are the closely related terms normally discussed when describing a P–E hysteresis.

$$E_c = \frac{E - E_r}{2},\ E_{bias} = \frac{E + E_r}{2} \quad (2)$$

However, in this work, the switching densities are plotted as a function of (E_r,E) because some important conclusion cannot be drawn from the plot versus (E_c,E_{bias}). Nonetheless, the latter

DOI: 10.1021/acsami.5b05773
ACS Appl. Mater. Interfaces 2015, 7, 20224−20233

notation was used to describe the results in the text similar to what is common for describing $P-E$ hystereses.

Another important point discussed in literature, is the following: Besides the derivation of information about switching domains, a FORC measurement can also be used to obtain information about reversible processes. Along the diagonal $E_r = E$ (or $E_{bs} = E_s$), the switching and backswitching field are the same, which hints on reversible contributions to the FORC density. Experimental[22] and mathematical[24,25] approaches exist to probe these contributions. The former use a small-signal superimposed to the large signal of the FORCs. Similar to a small-signal capacitance−voltage measurement, maxima in the response signal do not stem from switching domains, but from the lattice and oscillations of domain walls.[22] The mathematical approaches numerically calculate a switching density around the diagonal $E_r = E$ ($E_{bs} = E_s$) and defines the outcome as reversible contributions. In both approaches, difficulties result from the definition of what is "reversible". The Preisach model itself formally allows also hysterons with a rather small difference between E_s and E_{bs}. The measure to distinguish between "irreversible" and "reversible" are the field amplitude of the small signal excitation or the grid that samples the (E_r,E)-plane. The big advantage of the experimental approach results from the fact, that the small-signal is usually integrated over several periods and thus depends on reversibility, which is not the case for the response extracted from the mathematical approach. However, in either case, the definition of "reversible" can be debated due to the arbitrary choice of a legitimate field difference between E_{bs} and E_s. In the present work, it should suffice to know that phenomena around this diagonal, which are always clearly distinguished from the main peak(s), are due to either these reversible phenomena or artifacts from the measurement itself.[25]

In the following section, the results of the FORC studies of wake-up, fatigue, and split-up are discussed.

RESULTS AND DISCUSSION

The wake-up effect was studied by adapting the procedure described in ref 15. FORCs were measured on a pristine capacitor and on further capacitors previously subjected to 10, 100,... rectangular switching cycles at 10 kHz and 4 MV/cm amplitude. Figure 3a shows the switching density and corresponding pinched P-E loop in the inset. It can be clearly seen that the pristine sample exhibits two oppositely biased regions, around +1.3 and −1.5 MV/cm with coercive fields of about 2.0 and 2.2 MV/cm, respectively. As Figure 3b shows, these peaks merge during cycling until after 1000 cycles only one maximum remains at nearly zero bias and with a slightly increased coercive field of 2.3 MV/cm (Figure 3c). This proves that the presence of internal bias fields in the pristine Sr:HfO_2 sample is similar to what was reported also for conventional ferroelectrics like lead zirconate titanate PZT[27,22] and also illustrated from a pure mathematical point of view.[28] As the insets show, the remanent and maximum polarization increases during this initial stage of the field cycling treatment indicating the activation of initially nonswitching domains (or the creation of additional ferroelectric phase fractions).

Going to a higher number of field cycles, the onset of fatigue is observed. This effect was studied in a similar way by comparing the FORC results of the sample directly after wake-up (Figure 3b) to a fatigued sample. Figure 4a shows the evolution of the $2P_r$ (two times the remanent polarization

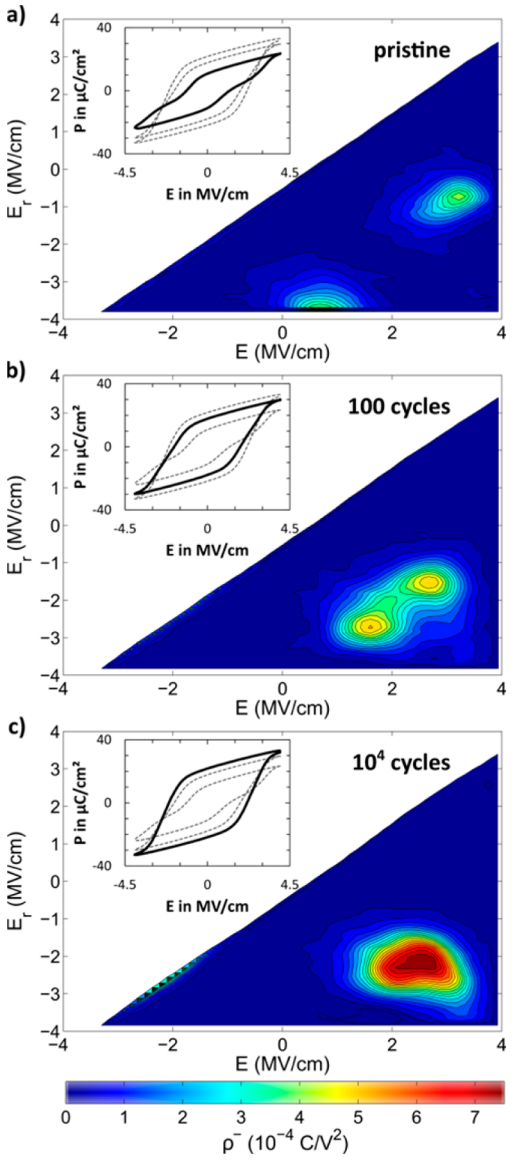

Figure 3. Wake-up for 4 MV/cm amplitude: Experimental switching density determined for (a) a pristine capacitor, (b) after 100, and (c) after 1×10^4 rectangular switching cycles. The insets show the respective polarization hystereses (extracted from each last FORC cycle) for comparison. The solid line of each inset is the hysteresis for the accompanying switching density plot, whereas the dashed lines are the respective two other hystereses for comparison.

obtained from the last FORC-sweep from positive to negative saturation and back) and the peak height(s) ρ_{max} of the switching density versus the number of switching cycles for a field amplitude of 3 MV/cm. Even after the peak in $2P_r$, the trend of peak merging persists as evidenced by the still growing maximum value of ρ_{max}. This might point to different mechanisms being involved in the wake-up and fatigue effect, which is in accordance to what was speculated due to the different activation energies and their frequency dependences.[15] The switching densities and $P-E$ hystereses corresponding to the maximum in this curve (= end of wake-up; 1×10^4 cycles) and a clearly fatigued state (1×10^6 cycles) of the sample are depicted in Figure 4b, c, respectively. Domain wall pinning[18] as one mechanism proposed to explain fatigue, should give rise to an increase of reversible contributions i.e. the observation of

DOI: 10.1021/acsami.5b05773
ACS Appl. Mater. Interfaces 2015, 7, 20224−20233

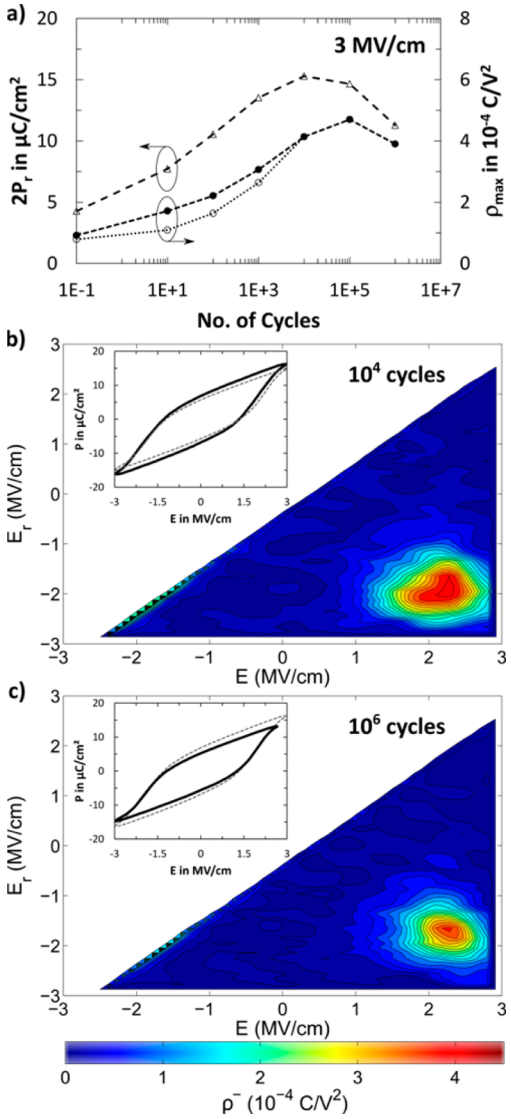

Figure 4. Fatigue for 3 MV/cm amplitude: (a) Evolution of $2P_r$ and (b) the peak height(s) of the switching density with the number of switching cycles and corresponding switching density plots obtained for 10^4 cycles, i.e. after wake-up and after 1×10^6 cycles (c), i.e., in a fatigued state. The solid line of each inset is the hysteresis for the accompanying switching density plot, whereas the dashed line is the respective other hystereses for comparison.

maxima close to the diagonal $E_r = E$, which is not clearly supported by our data. Comparing the two pseudocolor plots, it can be seen that the maximum becomes less pronounced and only slightly changes its position in E_c and surprisingly also in E_{bias}. The coercive field stays nearly constant at 2.0 MV/cm and is accompanied by a slight shift from 0.2 MV/cm toward a bias field of 0.3 MV/cm. This bias shift is not necessarily expected, but it points to a further evolution of asymmetry in the nominally symmetric TiN−Sr:HfO_2−TiN capacitor stack. An imprint effect caused by the measurement itself is negligible comparing the only 60 FORC sweeps to the 1×10^6 cycles before. An initial asymmetry (i.e., before wake-up cycling) in nominally symmetric capacitors was reported by several groups before.[29,30,17,31] For TaN electrodes it was argued, that differently oxidized interfaces between HfO_2 and the electrodes result in a higher O vacancy accumulation at the bottom electrode.[29,30] This high concentration of positive charges was concluded to favor the positive side of the ferroelectric dipoles to be directed toward this electrode.[30] For TiN-electrodes, a similar effect was also proposed.[17] If a similar mechanism is involved here, a preferential movement of O vacancies toward one of the electrodes during cycling could be concluded. Besides vacancy movement, differently strong charge injection through or into the different Ti−O−N layers[29,32] near the electrodes might also be an effect that results in the change from a symmetric to an asymmetric situation again. During wake-up, a redistribution or charging/discharging of defects states inside the HfO_2 might first give rise to the evolution of the switching density toward a more symmetric situation. Once this redistribution is established and complete, a second mechanism leading to the observed less pronounced asymmetry becomes visible. Different activation energies for fatigue and wake-up also support the coexistence of two superimposed effects.[15]

Both, wake-up and fatigue are detrimental for the operation of a capacitor based ferroelectric memory.[33,37] These memories typically consist of large arrays of single memory cells. In each of the cells, an access transistor is used to select the cell to be read or written at a certain point of the memory operation. The states "1" and "0" are stored as the polarization directions of the ferroelectric in the storage capacitor of the cell. Writing is done by applying either a positive or a negative field across the capacitor to switch it into the respective state. For the read process, a pulse of the same amplitude but always only one and the same polarity is applied. Depending on the polarization state, either a high (switching case) or a low (nonswitching case) amount of displaced charge can be sensed.[33] The remanent polarization defines the ratio of the displaced charge in the switching and nonswitching case during the read operation of the two states of the memory. To achieve a reliable and scalable memory, $2P_r$ has to be of reasonable magnitude (e.g., >6 $\mu C/cm^2$) and stable over the number of switching cycles.[38] Depending on the targeted type of memory, additional requirements have to be met. For the ambitious aim of a nonvolatile random access memory (RAM), unlimited cyclic endurance (in practice, $>1 \times 10^{15}$ cycles) and data retention (typical criterion, >10 years) have to be guaranteed.[33] The so-called "voltage−time dilemma"[33] limits not only the achievable switching times but also the simultaneous optimization of the device toward maximum retention and endurance

(1) A long data retention is based on a high barrier between the two stable states of the ferroelectric's double-well potential and corresponds to a high coercive voltage/field, which from the retention perspective should be as high as possible.
(2) This also increases the voltage necessary for fast switching or the other way around: At a given operation voltage, the switching process becomes slower as the barrier increases.
(3) A high field across the ferroelectric causes a faster degradation due to defect generation/movement, which results in faster dielectric breakdown. Also the mechanisms leading to polarization fatigue might be enhanced.
(4) Finally, the higher the switching voltage for a given charge carrier, the higher the energy consumption. Even, if the energy consumption for a single switching process itself is not critically increased, a higher voltage has to be provided by the peripheral circuitry of the memory cell.

DOI: 10.1021/acsami.5b05773
ACS Appl. Mater. Interfaces 2015, 7, 20224−20233

For a volatile type of RAM similar to, for example, a dynamic random access memory (DRAM), the retention criterion strongly relaxes to the second range.[33] Thus, the material development can be focused on maximizing the endurance and keeping the operation voltage as low as possible while still retaining a sufficient margin for the read operation. Such DRAM-like[39] devices based on ferroelectric hafnia have already been implemented utilizing a ferroelectric field effect transistor,[40] but also capacitor-based memory cells are conceivable. Because of the high coercive fields in the order 1 MV/cm for HfO_2-based ferroelectrics, dielectric breakdown is a limiting factor in the endurance data found in literature. The endurance could be increased by several orders of magnitude by operating the capacitors at reduced fields, i.e., in a sub-cycle.[41−43] Because of the high coercive field compared to, e.g., PZT, the performance in data retention[44,42] might be less critical even in a ferroelectric field effect transistor with much higher expected depolarization fields[45] than for a capacitor.

FORCs were used to exemplarily study the capabilities of the present Sr:HfO_2 sample to point out the limitation caused by wake-up and fatigue. Figure 5a shows plots of $2P_r$ vs the number of cycles for different field amplitudes. It can be seen, that for the highest amplitudes of 4.5 MV/cm, a $2P_r$ up to 47 $\mu C/cm^2$ can be achieved. However, the endurance is limited by dielectric breakdown to only around 1×10^2 cycles. Reducing the amplitude to 3.75 and 3.0 MV/cm causes a decrease of the maximum $2P_r$ margin by 8 and 32 $\mu C/cm^2$, respectively.

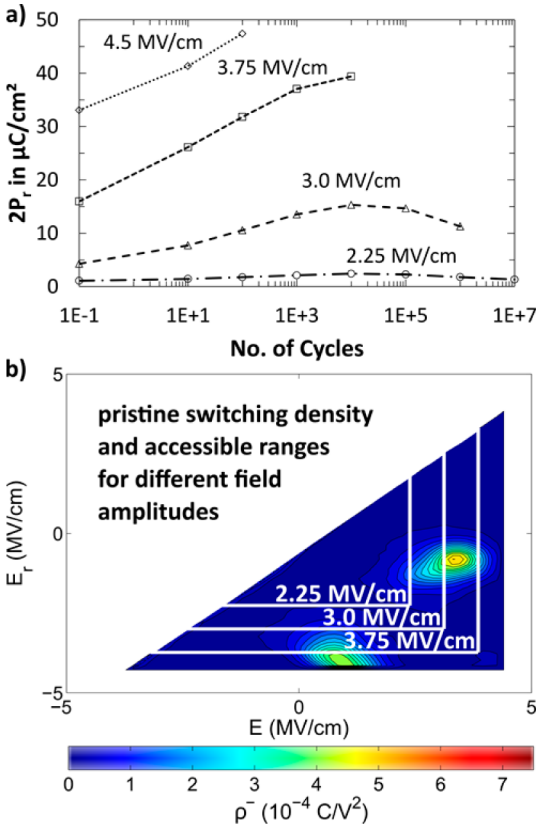

Figure 5. Optimization problem to solve: (a) Evolution of $2P_r$ for different field amplitudes as a function of the number of cycles and (b) switching density of the initial sample obtained with a FORC amplitude of 4.5 MV/cm). The triangular white frames represent the accessible range of domains for the respective lower field amplitudes.

Nonetheless, with these operating conditions, the capacitors are able to withstand 1×10^4 and 1×10^6 cycles, respectively, when cycled at 10 kHz. The initial $2P_r$ are about 40 and 30% of the maximum value. For 3.0 MV/cm, the onset of fatigue is clearly visible at 1×10^4 cycles and reduces the $2P_r$ value to about 70% before dielectric breakdown ends the lifetime of this capacitor. A further reduction of the amplitude to 2.25 MV/cm, which is still higher than the coercive fields in Figure 3, results in a higher endurance of 1×10^8 cycles and a lower variation of $2P_r$ between 45 and 50% of the maximum value achieved after 1×10^4 cycles. However, the tremendous drop of the maximum $2P_r$ to only 2.4 $\mu C/cm^2$ makes this operation condition unfavorable. So overall, none of the given conditions satisfied the criteria of a stable and reasonable high $2P_r$ over a noticeable amount of switching cycles. Of course, the frequency of 10 kHz used in this fundamental study is at least 3 orders of magnitude lower than what is of interest for an integrated device. A stretching of the curves in Figure 5a along the x-axis by at least the same factor is expected which relaxes the situation.

Nonetheless, the strong drop in the maximum $2P_r$ margin is still an issue and might seem a bit surprising, given that all used fields are well above the E_c values shown in Figure 3: For 2.25 MV/cm the maximum $2P_r$ was 2.4 instead of 47 $\mu C/cm^2$. Even for 3.0 MV, which is clearly above E_c, only 15 $\mu C/cm^2$ could be achieved. A simple description of the ferroelectric behavior with P_r and E_c is insufficient. Figure 5b illustrates the reason behind: 2.25 MV/cm is too low to reach to the maxima in the switching density. The domains of the upper right maximum are switched to negative polarization (if they have not been in this state already), but the switching to positive polarization cannot be achieved because the applied field is below the necessary switching field. For the domains of the maximum in the lower left part of the FORC density, the situation is the other way around: The domains are stuck in the positive polarization state once they are switched there. The field amplitude does not reach the back switching field. Thus, nearly zero domains take place in the endurance experiment once the first field cycle from 0 to +2.25 MV/cm, −2.25 MV/cm and back to 0 is completed. Also for 3.0 MV/cm the initial maxima in the switching density are outside the accessible range (white triangle), which explains the strong decrease of $2P_r$ in Figure 5a. Figure 5b clearly shows that the existence of two oppositely biased initial maxima in the switching density hampers a further optimization of the device toward lower switching fields. It impressively proves that the initial situation, which causes the wake-up effect, is critical for the operation of the envisaged memory application and has to be improved by optimized fabrication processes. Annealing could be a main knob,[9] but in-depth studies dedicated to the problem are still missing. In PZT-based commercial ferroelectric memories, the fatigue problem has been solved by (1) an optimization of the stoichiometry with respect to Pb content[34−36] and (2) using Ir or IrO_2 electrodes,[37] which do not pull oxygen out of the ferroelectric film. The potential role of the TiN electrodes in the wake-up effects was already discussed above. Thus, a proper choice of electrodes for HfO_2 could also be the solution to both fatigue and also the wake-up effect. Another perturbing effect for the operation of ferroelectric memories is the so-called "imprint", the shift of the polarization hysteresis toward one direction of the electric field.[37] It is the result of the stabilization of one state to the disadvantage of the other polarization direction. This effect is also related to (charged) defects and, applying this concept by analogy, the situation before wake-up

DOI: 10.1021/acsami.5b05773
ACS Appl. Mater. Interfaces 2015, 7, 20224−20233

could be called a "double-sided imprint". The solution of one of the phenomena might also solve or mitigate the issues with the other mechanisms. Besides processing, a short wake-up sequence with higher amplitude prior to low-voltage operation might be a workaround. But because it requires either an external cycling of all capacitors or the integration of a suitable periphery providing this high voltage on the chip, this solution seems less favorable.

In a third experiment, the split-up/merging phenomenon of transient current peaks was investigated. A sample after wake-up cycling (similar to Figure 3c) was subjected to 1×10^6 cycles at 2 V to induce the very pronounced pinching in the hysteresis (inset of Figure 6a) as the result of the split-up in the transient current peaks. After this subcycling treatment, a FORC measurement was performed to see the manifestation of the split-up effect. As can be seen from Figure 6a, the subcycling sequence resulted in two maxima similar to the situation before wake-up. After the split-up, there are clearly two regions with coercive fields of around 2.3 and 2.6 MV/cm and strongly different bias fields of +0.8 and −0.8 MV/cm, respectively, which is in contrast to the existing model mentioned in the introduction. That model was based on the assumption that static domains act as preferential locations for defects which cause an increased field to switch these domains in favor of the domains that took part in the switching during the subcycling sequence.[15] In such a case, two maxima aligned along the E_c' diagonal would be expected.[19] From the present measurements, the split-up/merging effect seems to be similar to the wake-up. It is, moreover, reversible by cycling with the higher amplitude. Figure 6b looks similar to Figure 3c again because it was obtained after subjecting the sample of Figure 6a to 1×10^4 cycles at 4 MV/cm again. Thus, an explanation similar to what was proposed for PZT might be tempting and an approach based on local imprint/internal bias fields could be used.[27,46] As the originally proposed model, this "imprint-like" explanation is in accordance with the evolution of the split-up with the number of subcycles shown in Figure S1 in the Supporting Information of ref 15. Nonetheless, the reported occurrence of multiple split-ups close to the fields used for subcycling still needs further investigation. Figure 6c shows the switching density after a subcycling treatment with first 1×10^6 cycles at 2.5 MV/cm and then 1×10^6 cycles at 1.5 MV/cm. Instead of only two maxima, four maxima are observed, which is in contrast to the former model approach presented in ref 15 which would require three maxima along the E_c'-axis. It should also be noted, that the slope of branches from saturation toward zero field in the $P-E$ hystereses did not strongly change. A change would have hinted to a different effective relative permittivity, i.e. changes in the dielectric properties (i.e., a hint to a phase change) of the ferroelectric or interfacial layers.

Figure 7 shows, how the results can be explained within the frame of a different local biasing of different domains of the sample as a result of one or more subcycling sequences. Figure 7a−c illustrate the Preisach plane and the polarization direction (up or down = positive or negative with respect to sign convention given by the electric field E) at different stages of the performed experiment for a single split-up (a subcycling sequence with one field amplitude). The horizontal and vertical lines indicate the amplitude of the subcycling field E_{sub} on the switching and backswitching field axis. The insets sketch the applied pulse train, where the highlighted pulses indicate the already performed fraction of the pulse train. Figure 7a shows the situation during the wake-up cycling with the high

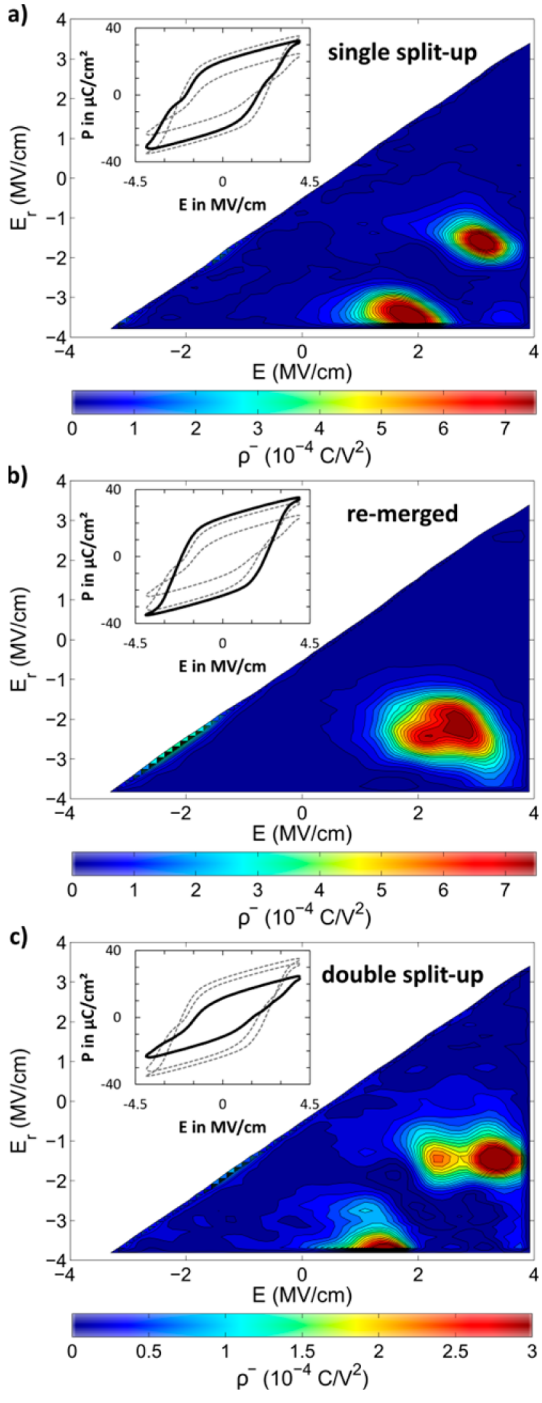

Figure 6. Split-up/merging for 4 MV/cm amplitude after wake-up treatment (see Figure 3a): Experimental switching density determined for (a) a capacitor subjected to 1×10^6 cycles of 2 MV/cm (split-up) amplitude, (b) the same capacitor after 1×10^4 merging cycles of 4 MV/cm amplitude, and (c) a capacitor subjected to a double split-up by subsequent cycling at 2.5 MV/cm and 1.5 MV/cm for 10^6 cycles each. Note the different pseudocolor-scale of (c). The solid line of each inset is the hysteresis for the accompanying switching density plot, whereas the dashed lines are the respective two other hystereses for comparison.

amplitude: All domains are steadily switched back and forth and at the end of the sequence, the switching density already shown in Figure 3c is obtained. The white outline is also drawn in Figure 7b−d as a reference. As the next step, a FORC measurement is performed leaving all domains switched to

DOI: 10.1021/acsami.5b05773
ACS Appl. Mater. Interfaces 2015, 7, 20224−20233

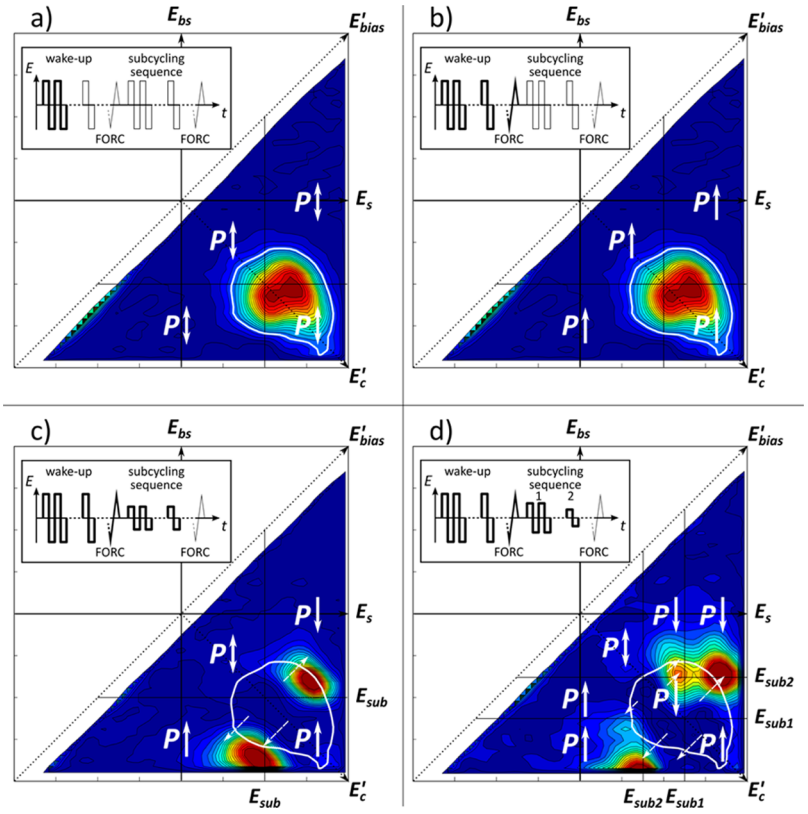

Figure 7. Evolution of the polarization state during the pulse train of the split-up experiments. See text for a detailed explanation of the manifestation of the split-up effect as a local imprint/internal biasing mechanism with (a−c) one and (d) two subcycling field(s).

positive polarization (Figure 7b) as a result of the applied field sweep sketched in Figure 2. For the sake of simplicity, the sketch is not 100% precise here since it treats the upper right quadrant not properly: The domains in this area should be switched to negative polarization, but virtually no domains exist in the region so it is treated similar to the neighboring regions below the E_s-axis.

Now the subcycling sequence follows. Figure 7c shows that all domains with E_{bs} and E_s below E_{sub} are steadily switched back and forth. The domains with an absolute $E_{bs} > E_{sub}$ (lower left and lower right part of Figure 7c) are stuck in the positive polarization state because they cannot be switched to negative polarization. In contrast, the domains with $E_{bs} < E_{sub}$ are switched to negative polarization during the first subcycle and for $E_s > E_{sub}$, the domains retain this negative polarization state during the whole remaining subcycling sequence (upper right part in Figure 7c). No changes to this situation occur during the whole subcycling sequence, but the high applied fields are likely to move or inject charges into the film during subcycling. This stabilizes the sketched situation and results in an imprint of the respective regions as sketched by the dashed arrows parallel to the bias field axis. Consequently, a split-up of the single maximum after wake-up into two oppositely biased maxima after the subcycling sequence is observed.

Figure 7d shows the corresponding—more complex—situation for a subcycling sequence with two different field amplitudes as a double split-up. As the sequence with the first (the higher) subcycling amplitude E_{sub1} starts, the domains in the lowest and most right part of the Preisach plane get stuck and only in the second subcycling sequence the domains of the next inner part of the Preisach plane are affected. These domains start at a lower E_c and start being subject to the imprint effect later in time and with a lower field amplitude E_{sub2} (charge movement/injection is less effective). This results in the occurrence of two maxima at higher E_c and higher E_{bias} and two at lower E_c and lower E_{bias}, as it is shown in Figure 6c. Two important details should be noted: (1) The asymmetry with respects to the diagonal E_c' in Figure 7d is not due to an asymmetric sample configuration. Even when interchanging the external wires to top and bottom electrode, the obtained switching densities look always like in Figure 7d. From the model, precisely this result is expected, because the central square with E_s and E_{bs} greater than E_{sub2} but smaller than E_{sub1} moved toward positive biased fields. (2) According to the proposed explanation, a maximum at zero E_{bias} and the lowest E_c should remain which corresponds to the domains steadily switched during the whole pulse train. In Figure 6a and 6c one might speculate that this is reflected in the slight plateau in the switching density around $E_r = -1.5$ MV/cm and $E = +1$ MV/cm, but its manifestation is too weak to take it as clear evidence. This hints to interactions between the domains (and/or moved charges/defects), which are of course not taken into account in this simple model but are highly likely in real films.

The FORC approach is not able to proof the movement/generation of defects or charges, but it proves similarities between the new class of hafnia and zirconia based ferroelectrics and conventional ferroelectrics. Nonetheless, material specific differences should be taken into account when interpreting the results. In PZT, pinched hysteresis are discussed to stem from diffusion of defects into charged, strained domain walls or dipole reorientation within the perovskite unit cell.[47] All of these mechanisms could in principle play a role for HfO_2/ZrO_2-based ferroelectric as well. In PZT, the reorienting dipoles within the unit cell stem from

DOI: 10.1021/acsami.5b05773
ACS Appl. Mater. Interfaces 2015, 7, 20224−20233

oxygen vacancies induced by acceptor doping. Because of the solubility limit of, for example, <1% (cationic ratio) for Fe doping of PZT ceramics,[48] the amount of oxygen vacancies induced by that doping is also limited to a similar range. For thin films, the solubility limit was reported to be increased to about 5%, but the charge neutrality is achieved by the creation of holes rather than by oxygen vacancies.[49] For HfO_2, ferroelectric properties have been reported for concentrations typically around 3−6% (dopant/[dopant + Hf]).[2] Moreover, even pure HfO_2 thin films fabricated by atomic layer or sputter deposition are to a certain extent substoichiometric[50] and thus, the overall concentration of oxygen vacancies is expected to be higher than for PZT. An additional difference arises from the fact that oxygen is the ion that switches in the unit cell. In PZT, it is the Zr or Ti ion that is surrounded by an octahedron of oxygen ions. The situation becomes even more complex, given the reports on the effect of oxygen vacancies on the stability of the ferroelectric phase compared to the competing paraelectric phases.[8,29] It was already pointed out, that the electric fields applied to HfO_2-based ferroelectric are at least 1 order of magnitude higher than for, for example, PZT and that HfO_2/ZrO_2 are known for their high oxygen mobility.[19] This gives rise to speculating about the movement of oxygen-related dipoles/defects through the whole film and not only within a unit cell or toward grain boundaries. Also a generation of new defects is supported by higher fields. An in situ study by transmission electron microscopy confirmed the generation and movement of oxygen and oxygen vacancies in a 10 nm thick HfO_2 film at similar conditions.[51] However, the redistribution/generation of charges or defects needs further investigations also via structural methods or simulations. Up to now, only one first simulation approach exists for HfO_2-based ferroelectrics:[52] Wake-up can be caused by an asymmetric distribution of charged defects at top and bottom electrode. These defects from the interfaces become redistributed into the volume of the ferroelectric during the peak merging as seen during the wake-up procedure. Fatigue was discussed as fairly symmetric generation of static defects and charging at both interfaces, which shield the electric field and thus, cause a decrease in switched polarization similar to a dead or passive layer effect discussed elsewhere.[53] The role of the TiN electrodes and the formation of a Ti−O−N layer was discussed already in the frame of the wake-up and fatigue effects.

CONCLUSIONS

In conclusion, switching density plots were obtained using the approach of first-order reversal curves (FORCs) for samples subjected to different field cycling sequences. The manifestations of three different phenomena were studied: (1) wake-up, (2) fatigue, and (3) merging after split-up by subcycling. All three phenomena are of crucial relevance for, for example, the application in ferroelectric memories. FORC measurements were shown to be a suitable method to gather deeper insights into the evolution of the switching behavior than a single dynamic hysteresis measurement would allow. The experiments on the wake-up effect showed that a pristine sample exhibits at least two distinct maxima in the switching density, which are biased against each other and merge together into one single maximum around zero bias field during field cycling. For even higher numbers of cycles, this maximum decreases and slightly shifts toward higher coercive fields, which is in accordance with a decreasing number of switchable domains and an impaired reversal of the remaining switchable domains. Even more importantly, it was demonstrated how both the fatigue and the wake-up effect are detrimental for the subcycle-operation of a capacitor based ferroelectric memory and that an optimization of the fabrication conditions is needed to achieve stable, low-voltage operating conditions with reasonable P_r and highest possible endurance. A solution to that optimization problem can only be provided by suitable fabrication processes that result in only one distinct maximum in the switching density, most favorably without internal bias field. Here, detailed studies are still missing. The alternative of a short wake-up sequence with higher amplitude prior to low-voltage operation would require an external cycling of all capacitors or the integration of a suitable periphery providing this high voltage on the chip and is, thus, not the most favorable workaround. Finally, the split-up/merging phenomenon was shown to be similar to the wake-up effect based on a local imprint/internal biasing mechanism. The originally claimed model proposed in a former publication[15] is not supported by the results. Indeed, the split-up is based on inducing differences between switching and nonswitching domains as formerly proposed, but the mechanism behind results in locally different bias fields rather than in changes of the coercive fields. A detailed description of how to explain the complex situation of multiple split-ups within the frame of local imprint/biasing was given. So on the one hand, this study evidences the potential of FORC for in-depth investigation of the field cycling related phenomena as it is required for future material optimization by adjusting the capacitor or transistor gate stacks and their preparation processes. On the other hand, it impressively illustrates the complexity of the interplay between ferroelectric domains and (charged) defects especially at comparably high electric fields of a few MV/cm. Similarities and differences of HfO_2 and PZT were discussed to stimulate the discussions about the underlying mechanisms and future work in this direction.

EXPERIMENTAL PROCEDURES

A Keithley 4200 SCS equipped with a pulse generator and an oscilloscope unit was used to apply the FORC sweeps and measure the displacement current as a voltage drop over a 50 Ω series resistor. This setup allowed up to one million samples and the realization of a 60 × 60 (E_r,E)-grid. The time between two measurement points was adjusted to the maximum voltage to ensure a comparable field ramp between 8 and 9 V/(cm s) for all FORCs. For data analysis a mathematically more robust procedure than the illustrative one described in section 2 was chosen, which is similar to what can be found in ref 21. For the analysis of the FORC data, a script was implemented in MATLAB (version R2011b). A polynomial surface of second-order was fitted to each data point (E_r,E) with smoothing on a 5 × 5 grid (equals a smoothing factor of 2^{21}). Also the rectangular cycling sequences between the FORC measurements were applied using the Keithley 4200 SCS and started, as Figure 7 illustrates, at 0 MV/cm with a positive pulse and ended at 0 MV/cm after a negative Pulse. The times between cycling sequence and measurement were in the range of a few seconds because of the change between different programs. The obtained FORC distributions were stable for at least several hours if the sample was not subjected to electric field cycling.

AUTHOR INFORMATION

Corresponding Author

*E-mail: tony.schenk@namlab.com.

DOI: 10.1021/acsami.5b05773
ACS Appl. Mater. Interfaces 2015, 7, 20224−20233

Funding

This work was funded by the German Research Foundation (Deutsche Forschungsgemeinschaft) within the project "Inferox" (MI 1247/11−1).

Notes

The authors declare no competing financial interest.

■ ACKNOWLEDGMENTS

Mihaela Popovici from Imec, Belgium, is gratefully acknowledged for the deposition of the TiN-Sr:HfO_2−TiN stacks.

■ REFERENCES

(1) Böscke, T. S.; Müller, J.; Bräuhaus, D.; Schröder, U.; Böttger, U. Ferroelectricity in Hafnium Oxide Thin Films. *Appl. Phys. Lett.* **2011**, *99*, 102903.

(2) Schroeder, U.; Yurchuk, E.; Müller, J.; Martin, D.; Schenk, T.; Polakowski, P.; Adelmann, C.; Popovici, M. I.; Kalinin, S. V.; Mikolajick, T. Impact of Different Dopants on the Switching Properties of Ferroelectric Hafniumoxide. *Jpn. J. Appl. Phys.* **2014**, *53*, 08LE02.

(3) Müller, J.; Böscke, T. S.; Bräuhaus, D.; Schröder, U.; Böttger, U.; Sundqvist, J.; Kücher, P.; Mikolajick, T.; Frey, L. Ferroelectric $Zr_{0.5}Hf_{0.5}O_2$ Thin Films for Nonvolatile Memory Applications. *Appl. Phys. Lett.* **2011**, *99*, 112901.

(4) Müller, J.; Böscke, T. S.; Schröder, U.; Mueller, S.; Bräuhaus, D.; Böttger, U.; Frey, L.; Mikolajick, T. Ferroelectricity in Simple Binary ZrO_2 and HfO_2. *Nano Lett.* **2012**, *12*, 4318−4323.

(5) Clima, S.; Wouters, D. J.; Adelmann, C.; Schenk, T.; Schroeder, U.; Jurczak, M.; Pourtois, G. Identification of the Ferroelectric Switching Process and Dopant-Dependent Switching Properties in Orthorhombic HfO_2: A First Principles Insight. *Appl. Phys. Lett.* **2014**, *104*, 092906.

(6) Reyes-Lillo, S. E.; Garrity, K. F.; Rabe, K. M. Antiferroelectricity in Thin Film ZrO_2 from First Principles. *Phys. Rev. B: Condens. Matter Mater. Phys.* **2014**, *90*, 140103(R).

(7) Huan, T. D.; Sharma, V.; Rossetti, G. A., Jr.; Ramprasad, R. Pathways Towards Ferroelectricity in Hafnia. *Phys. Rev. B: Condens. Matter Mater. Phys.* **2014**, *90*, 064111.

(8) Materlik, R.; Künneth, C.; Kersch, A. The Origin of Ferroelectricity in $Hf_{0.5}Zr_{0.5}O_2$: A Computational Investigation and a Surface Energy Model. *J. Appl. Phys.* **2015**, *117*, 134109.

(9) Park, M. H.; Kim, H. J.; Kim, Y. J.; Lee, W.; Moon, T.; Hwang, C. S. Evolution of Phases and Ferroelectric Properties of Thin $Hf_{0.5}Zr_{0.5}O_2$ Films According to the Thickness and Annealing Temperature. *Appl. Phys. Lett.* **2013**, *102*, 242905.

(10) Lomenzo, P. D.; Zhao, P.; Takmeel, Q.; Moghaddam, S.; Nishida, T.; Nelson, M.; Fancher, C. M.; Grimley, E. D.; Sang, X.; LeBeau, J. M.; Jones, J. L. Ferroelectric Phenomena in Si-Doped HfO_2 Thin Films with TiN and Ir Electrodes. *J. Vac. Sci. Technol., B: Nanotechnol. Microelectron.: Mater., Process., Meas., Phenom.* **2014**, *32*, 03D123.

(11) Shimizu, T.; Yokouchi, T.; Shiraishi, T.; Oikawa, T.; Sankara Rama Krishnan, P. S.; Funakubo, H. Study on the Effect of Heat Treatment Conditions on Metalorganic-Chemical-Vapor-deposited Ferroelectric $Hf_{0.5}Zr_{0.5}O_2$ Thin Film on Ir Electrode. *Jpn. J. Appl. Phys.* **2014**, *53*, 09PA04.

(12) Mikolajick, T.; Müller, S.; Schenk, T.; Yurchuk, E.; Slesazeck, S.; Schröder, U.; Flachowsky, S.; van Bentum, R.; Kolodinski, S.; Polakowski, P.; Müller, J. Doped Hafnium Oxide − An Enabler for Ferroelectric Field Effect Transistors. *Adv. Sci. Technol.* **2014**, *95*, 136−145.

(13) Chernikova, A.; Kozodaev, M.; Markeev, A.; Matveev, Yu.; Negrov, D.; Orlov, O. Confinement-free Annealing Induced Ferroelectricity in $Hf_{0.5}Zr_{0.5}O_2$ Thin Films. *Microelectron. Eng.* **2015**, *147*, 15−18.

(14) Sang, X.; Grimley, E. D.; Schenk, T.; Schroeder, U.; LeBeau, J. M. On the Structural Origins of Ferroelectricity in HfO_2 Thin Films. *Appl. Phys. Lett.* **2015**, *106*, 162905.

(15) Schenk, T.; Schroeder, U.; Pešić, M.; Popovici, M.; Pershin, Y. V.; Mikolajick, T. Electric Field Cycling Behavior of Ferroelectric Hafnium Oxide. *ACS Appl. Mater. Interfaces* **2014**, *6*, 19744−19751.

(16) Menou, N.; Muller, C.; Baturin, I. S.; Shur, V. Y.; Hodeau, J.-L. Polarization Fatigue in $PbZr_{0.45}Ti_{0.55}O_3$-based Capacitors Studied from High Resolution Synchrotron X-ray Diffraction. *J. Appl. Phys.* **2005**, *97*, 064108.

(17) Zhou, D.; Xu, J.; Li, Q.; Guan, Y.; Cao, F.; Dong, X.; Müller, J.; Schenk, T.; Schröder, U. Wake-up Effects in Si-doped Hafnium Oxide Ferroelectric Thin Films. *Appl. Phys. Lett.* **2013**, *103* (19), 192904.

(18) Tagantsev, A. K.; Stolichnov, I.; Colla, E. L.; Setter, N. Polarization Fatigue in Ferroelectric Films: Basic Experimental Findings, Phenomenological Scenarios, and Microscopic Features. *J. Appl. Phys.* **2001**, *90*, 1387−1402.

(19) Schenk, T.; Yurchuk, E.; Mueller, S.; Schroeder, U.; Starschich, S.; Böttger, U.; Mikolajick, T. About the Deformation of Ferroelectric Hystereses. *Appl. Phys. Rev.* **2014**, *1*, 041103.

(20) Preisach, F. Über die Magnetische Nachwirkung. *Eur. Phys. J. A* **1935**, *94*, 277−302.

(21) Pike, C. R.; Roberts, A. P.; Verosub, K. L. Characterizing Interactions in Fine Magnetic Particle Systems Using First Order Reversal Curves. *J. Appl. Phys.* **1999**, *85*, 6660−6667.

(22) Cima, L.; Laboure, E.; Muralt, P. Characterization and Model of Ferroelectrics Based on Experimental Preisach Density. *Rev. Sci. Instrum.* **2002**, *73*, 3546−3552.

(23) Mitoseriu, L.; Stoleriu, L.; Stancu, A.; Galassi, C.; Buscaglia, V. First Order Reversal Curves Diagrams for Describing Ferroelectric Switching Characteristics. *Process. Appl. Ceram.* **2009**, *3*, 3−7.

(24) Fujii, I.; Hong, E.; Trolier-McKinstry, S. Thickness Dependence of Dielectric Nonlinearity of Lead Zirconate Titanate Films, Ultrasonics. *IEEE Trans. Ultrason., Ferroelect., Freq. Control* **2010**, *57* (8), 1717−1723.

(25) Fujii, I.; Trolier-McKinstry, S.; Nies, C. Effect of Grain Size on Dielectric Nonlinearity in Model BaTiO3-Based Multilayer Ceramic Capacitors. *J. Am. Ceram. Soc.* **2011**, *94* (1), 194−199.

(26) Stancu, A.; Ricinschi, D.; Mitoseriu, L.; Postolache, P.; Okuyama, M. First-Order Reversal Curves Diagrams for the Characterization of Ferroelectric Switching. *Appl. Phys. Lett.* **2003**, *83*, 3767−3769.

(27) Carl, K.; Hardtl, K. H. Electrical After-Effects in $Pb(Ti,Zr)O_3$ Ceramics. *Ferroelectrics* **1977**, *17* (1), 473−486.

(28) Robert, G.; Damjanovic, D.; Setter, N. Preisach Modeling of Ferroelectric Pinched Loops. *Appl. Phys. Lett.* **2000**, *77* (26), 4413−4415.

(29) Hoffmann, M.; Schroeder, U.; Schenk, T.; Shimizu, T.; Funakubo, H.; Sakata, O.; Pohl, D.; Drescher, M.; Adelmann, C.; Materlik, R.; Kersch, A.; Mikolajick, T. Stabilizing the Ferroelectric Phase in Doped Hafnium Oxide. *J. Appl. Phys.* **2015**, *118* (7), 072006.

(30) Lomenzo, P. D.; Takmeel, Q.; Zhou, C.; Fancher, C. M.; Lambers, E.; Rudawski, N. G.; Jones, J. L.; Moghaddam, S.; Nishida, T. TaN Interface Properties and Electric Field Cycling Effects on Ferroelectric Si-doped HfO_2 Thin Films. *J. Appl. Phys.* **2015**, *117*, 134105.

(31) Mueller, S.; Adelmann, C.; Singh, A.; Van Elshocht, S.; Schroeder, U.; Mikolajick, T. Ferroelectricity in Gd-doped HfO_2 Thin Films. *ECS J. Solid State Sci. Technol.* **2012**, *1*, N123−N126.

(32) Weinreich, W.; Reiche, R.; Lemberger, M.; Jegert, G.; Müller, J.; Wilde, L.; Teichert, S.; Heitmann, J.; Erben, E.; Oberbeck, L.; Schröder, U.; Bauer, A. J.; Ryssel, H. *Microelectron. Eng.* **2009**, *86* (7), 1826−1829.

(33) Waser, R. *Nanoelectronics and Information Technology: Advanced Electronic Materials and Novel Devices*, 3rd ed.; Wiley−VCH: Weinheim, Germany, 2005.

(34) Park, Y.; Jeong, K. W.; Song, J. T. Effect of Excess Pb on Fatigue Properties of PZT Thin Films Prepared by RF-Magnetron Sputtering. *Mater. Lett.* **2002**, *56* (4), 481−485.

DOI: 10.1021/acsami.5b05773
ACS Appl. Mater. Interfaces 2015, 7, 20224−20233

(35) Shturman, I.; Shter, G. E.; Etin, A.; Grader, G. S. Effect of $LaNiO_3$ Electrodes and Lead Oxide Excess on Chemical Solution Deposition Derived $Pb(Zr_xTi_{1-x})O_3$ Films. *Thin Solid Films* **2009**, *517* (8), 2767−2774.
(36) Lou, X. J. Polarization fatigue in ferroelectric thin films and related materials. *J. Appl. Phys.* **2009**, *105* (2), 024101.
(37) Scott, J. F. *Ferroelectric Memories*; Springer-Verlag: Berlin, 2000.
(38) Chu, F.; Davenport, T. *The Endurance Performance of 0.5μm FRAM Products*; Ramtron International Corporation: Colorado Springs, CO; http://www.digikey.com/Web%20Export/Supplier%20Content/ramtron-1140/pdf/ramtron-tech-fram-endurance.pdf?redirected=1
(39) Ma, T. P. FEDRAM: A Capacitor-less DRAM Based on Ferroelectric-Gated Field-Effect Transistor. In *2014 IEEE 6th International Memory Workshop (IMW)*; Taipei, Tawain, May18−21, 2014 ; IEEE: Piscataway, NJ, 2014 10.1109/IMW.2014.6849350.
(40) Cheng, C.-H.; Chin, A. Low-Leakage-Current DRAM-Like Memory Using a One-Transistor Ferroelectric MOSFET With a Hf-Based Gate Dielectric. *IEEE Electron Device Lett.* **2014**, *35*, 138−140.
(41) Mueller, S.; Summerfelt, S. R.; Muller, J.; Schroeder, U.; Mikolajick, T. Ten-Nanometer Ferroelectric Films for Next-Generation FRAM Capacitors. *IEEE Electron Device Lett.* **2012**, *33*, 1300−1302.
(42) Mueller, S.; Muller, J.; Schroeder, U.; Mikolajick, T. Reliability Characteristics of Ferroelectric Thin Films for Memory Applications. *IEEE Trans. Device Mater. Reliab.* **2013**, *13*, 93−97.
(43) Polakowski, P.; Riedel, S.; Weinreich, W.; Rudolf, M.; Sundqvist, J.; Seidel, K.; Muller, J. Ferroelectric Deep Trench Capacitors Based on Al:HfO_2 for 3D Nonvolatile Memory Applications. In *2014 IEEE 6th International Memory Workshop (IMW)*; Taipei, Taiwan, May 18−21, 2014 ; IEEE: Piscataway, NJ, 201410.1109/IMW.2014.6849367.
(44) Müller, J.; Böscke, T. S.; Schröder, U.; Hoffmann, R.; Mikolajick, T.; Frey, L. Nanosecond Polarization Switching and Long Retention in a Novel MFIS-FET Based on Ferroelectric HfO_2. *IEEE Electron Device Lett.* **2012**, *33*, 185−187.
(45) Ma, T.-P.; Han, J.-P. Why is Nonvolatile Ferroelectric Memory Field-Effect Transistor Still Elusive? *IEEE Electron Device Lett.* **2002**, *23*, 386−388.
(46) Morozov, M. I.; Damjanovic, D. Hardening-Softening Transition in Fe-doped $Pb(Zr,Ti)O_3$ Ceramics and Evolution of the Third Harmonic of the Polarization Response. *J. Appl. Phys.* **2008**, *104*, 034107.
(47) Damjanovic, D. In *The Science of Hysteresis: Hysteresis in Materials*; Bertotti, G., Mayergoyz, I. D., Eds.; Academic Press: Kidlington, U.K., 2006; Vol. 3, Chapter 4, pp 337−465.
(48) Erdem, E.; Eichel, R. A.; Fetzer, C.; Dé zsi, I.; Lauterbach, S.; Kleebe, H. J.; Balogh, A. G. Site of Incorporation and Solubility for Fe Ions in Acceptor-Doped PZT Ceramics. *J. Appl. Phys.* **2010**, *107* (5), 054109.
(49) Klissurska, R. D.; Brooks, K. G.; Setter, N. Effect of Dopants on the Crystallization Mechanism of PZT Thin Films. *Ferroelectrics* **1999**, *225* (1), 327−334.
(50) Gavartin, J. L.; Muñoz Ramo, D.; Shluger, A. L.; Bersuker, G.; Lee, B. H. Negative Oxygen Vacancies in HfO_2 as Charge Traps in High-k Stacks. *Appl. Phys. Lett.* **2006**, *89* (8), 2908.
(51) Li, C.; Yao, Y.; Shen, X.; Wang, Y.; Li, J.; Gu, C.; Yu, R. Dynamic Observation of Oxygen Vacancies in Hafnia Layer by In-Situ Transmission Electron Microscopy. *Nano Res.* **2015**, DOI: 10.1007/s12274-015-0857-0.
(52) Pešić, M.; Slesazeck, S.; Müller, S.; Schenk, T.; Schroeder, U.; Mikolajick, T.Modeling of Charge Trapping influence on the Ferroelectric Switching Behavior of Doped HfO_2. In *European Materials Research Society 2015 Spring Meeting*; Lille-Euralille, France, May 11−15, 2015 ; European Materials Research Society: Strasbourg, France, 2015.
(53) Tagantsev, A. K.; Landivar, M.; Colla, E.; Setter, N. Identification of Passive Layer in Ferroelectric Thin Films from their Switching Parameters. *J. Appl. Phys.* **1995**, *78*, 2623−2630.

DOI: 10.1021/acsami.5b05773
ACS Appl. Mater. Interfaces 2015, 7, 20224−20233